Available online at www.sciencedirect.com

ScienceDirect

Physics Procedia 64 (2015) 4 – 18

Physics Procedia

Scientific Workshop on Nuclear Fission dynamics and the Emission of Prompt Neutrons and Gamma Rays, THEORY-3

On microscopic energy corrections around scission configuration

Krzysztof Pomorski[a,*], Bożena Nerlo-Pomorska[a]

[a]*Theoretical Physics Department, Maria Curie Skłodowska University, Lublin, Poland*

Abstract

The spontaneous fission of actinides is analysed by the macroscopic - microscopic method based on the Lublin Strasbourg Drop model and the two deformed Nilsson wells or Yukawa folded single particle potentials. The microscopic corrections are obtained within the Strutinsky prescription and the BCS theory. In the scission point the shell correction possess the additive property but this is not true for pairing correlations during asymmetric fission . Here the shape dependent pairing force of the δ or Gogny type should be used and the pairing strength should grow with increasing deformation of fissioning nucleus. The examples of spontaneous fission results are presented. The possibility of β decay accompanying the spontaneous fission is noticed.

Peer-review under responsibility of the European Commission, Joint Research Centre – Institute for Reference Materials and Measurements

Keywords: nuclear fission; scission point; barrier heights; shell effects; life-times;
PACS: 24.75.+i, 25.85.-w, 21.10.Pc, 21.10.Tg

1. Introduction

After 75 years from the discovery of nuclear fission it is worth to remain the names of scientists: Otto Hahn, Fritz Strassmann, Lisa Meitner and Otto Frisch, who had discovered this phenomenon (Hahn and Strassmann, 1939) and began the long way of it's explanation (Meitner and Frisch, 1939). The first quantitative description of the fission process was proposed also in 1939 by Niels Bohr and John A. Wheeler (Bohr and Wheeler, 1939). Till now the mechanism of the nuclear, even spontaneous, fission is not fully understood. The life-times with respect of this decay are not well reproduced by any theory. Also the origin of asymmetric fission demands better descriptions. Similarly the theoretical description of the kinetic energy distribution of fission fragments needs further studies of the scission point configuration and the neck rupture mechanism. The crucial quantities influencing all these doubts are the shell and pairing correlations in the region of the scission point of the fission barrier.

* Corresponding author. Tel.: +048-81-537-6141 ; fax: +048-81-537-6190.
E-mail address: Krzysztof.Pomorski@umcs.pl

Peer-review under responsibility of the European Commission, Joint Research Centre – Institute for Reference Materials and Measurements
doi:10.1016/j.phpro.2015.04.002

The Strutinsky method was used to evaluate the shell correction in the fissioning nucleus and its fragments. It was shown that the sum of the shell corrections of the both fragments is nearly equal to the shell correction evaluated in the mother nucleus even for asymmetric fission.

The pairing correlation were evaluated using the BCS approximation with the monopole pairing force for the mother nucleus and the both fragments. The additive property is not true for the pairing correction, by asymmetric fission, where the pairing energy of the total system differs from the sum of the pairing energies of the fragments.

One has to use the δ-pairing or Gogny force instead of the monopole force in almost separated system. The shape dependent force will switch off the pairing correlations between orbitals in different fragments. The average pairing energy reproducing the masses of the fragments after scission should grow with deformation.

The paper is organised in the following way. We begin the article with presentation of a modern version of the liquid drop formula, namely the Lublin Strasbourg Drop (LSD) model (Pomorski and Dudek, 2003), which reproduces well the nuclear masses and the fission barrier heights. Then, we shall present the shell and pairing corrections at large deformations close to the scission point of the fissioning nucleus and examine the influence of the average pairing energy on the fission barrier heights of light nuclei with $A \approx 100$. In addition, we show that the β-stable nuclei lose their stability at large deformations what can lead to β-decays accompanying to fission. The conclusions will be drawn in the end of the paper.

2. Macroscopic-microscopic theory

2.1. Macroscopic part of the binding energy

Following the idea of Meitner and Frisch (Meitner and Frisch, 1939) Bohr and Wheeler have assumed that the liquid drop formula consists of the volume energy, and the deformation dependent surface and Coulomb energy terms (Bohr and Wheeler, 1939):

$$E_{LD}(\{\alpha_l\}) = E_{\rm vol} + E_{\rm surf}(\{\alpha_l\}) + E_{\rm Coul}(\{\alpha_l\}) = a_{\rm vol}A + a_{\rm surf}A^{2/3}B_{\rm surf}(\{\alpha_l\}) + \frac{e^2Z^2}{r_0A^{1/3}}B_{\rm Coul}(\{\alpha_l\}), \tag{1}$$

where $\{\alpha_l\}$, called deformation parameters, is a set of expansion coefficients of nuclear radius in Legendre polynomials P_l series

$$R(\theta) = R_0\left(1 + \sum_{l=0}^{\infty}\alpha_l P_l(\theta)\right). \tag{2}$$

Here R_0 is radius of a spherical nucleus.

Bohr and Wheeler have shown that the saddle point of the liquid drop energy function in the $\{\alpha_l\}$ deformation parameters space appears at large deformation α_2 and the fission barrier occurs when the fissility parameter

$$x = \frac{E_{\rm Coul}(0)}{2E_{\rm surf}(0)} \approx \frac{Z^2}{50A}{\rm MeV} \tag{3}$$

is smaller than 1, what is clearly seen when one expands the relative to sphere surface and Coulomb energies in the Taylor series with respect to the deformation parameters:

$$B_{\rm surf} = 1 + \frac{2}{5}\alpha_2^2 + \frac{5}{7}\alpha_3^2 + \dots \ ; \qquad B_{\rm Coul} = 1 - \frac{1}{5}\alpha_2^2 - \frac{10}{49}\alpha_3^2 - \dots \tag{4}$$

The shell effects in the deformed macroscopic potential energy surface was included in 1966 by Myers and Swiatecki who have proposed a phenomenological formula for the shell correction energy (Myers and Swiatecki, 1969,1974) what has allowed them, after refitting of the liquid drop formula parameters, to reproduce with a good accuracy the known at that time nuclear masses. After appearance of this first macroscopic-microscopic model (Myers and Swiatecki, 1966) several more complex macroscopic formulae containing more adjustable parameters were developed. One can count here the droplet model (Myers and Swiatecki, 1969,1974), the Yukawa-plus-exponential anzatz (Krappe et al., 1979), the finite-range droplet model (Moller, 1988) or the Thomas-Fermi theory (Myers and Swiatecki, 1996). Surprisingly, it was shown in Ref. (Pomorski and Dudek, 2003) that simple liquid drop formula containing the surface

curvature term is able to reproduce both the experimental binding energies and the fission barrier height with even better accuracy that the above more complex models when one uses the same microscopic energy corrections. This Lublin-Strasbourg-Drop (LSD) mass formula (Pomorski and Dudek, 2003) has the following form:

$$\begin{aligned} M(Z,N\,;\mathrm{def}) = {} & ZM_{\mathrm{H}} + NM_{\mathrm{n}} - b_{\mathrm{elec}}\,Z^{2.39} + b_{\mathrm{vol}}\,(1-\kappa_{\mathrm{vol}}\,I^2\,)\,A + b_{\mathrm{surf}}\,(1-\kappa_{\mathrm{surf}}\,I^2\,)\,A^{2/3}B_{\mathrm{surf}}(\mathrm{def}) \\ & + b_{\mathrm{cur}}\,(1-\kappa_{\mathrm{cur}}\,I^2\,)\,A^{1/3}B_{\mathrm{cur}}(\mathrm{def}) + \tfrac{3}{5}\,\tfrac{e^2Z^2}{r_0^{ch}A^{1/3}}\,B_{\mathrm{Coul}}(\mathrm{def}) - C_4\,\tfrac{Z^2}{A} + E_{\mathrm{micr}}(Z,N;\mathrm{def}) + E_{\mathrm{cong}}(Z,N)\,. \end{aligned} \tag{5}$$

where the congruence energy E_{cong} is defined in Ref. (Myers and Swiatecki, 1997) and the microscopic part of the binding energy E_{micr} consists of the shell $\delta E_{\mathrm{shell}}$ and pairing δE_{pair} energy corrections

$$E_{\mathrm{micr}}(Z,A;\mathrm{def}) = +\delta E_{\mathrm{shell}}(Z,A;\mathrm{def}) + \delta E_{\mathrm{pair}}(Z,A;\mathrm{def})\,, \tag{6}$$

One can obtain the microscopic energy corrections using the Nilsson (Nilsson, 1955; Nilsson et al. , 1969), the Saxon-Woods (Woods and Saxon, 1954) or the Yukawa-folded (Bolsterli et al., 1972) single-particle potentials and the Strutinsky method to evaluate the shell energy corrections (Strutinsky, 1967,1968; Nilsson et al. , 1969) while the BCS theory is used to get the pairing correlations energy(Bardeen et al., 1957; Nilsson et al. , 1969).

All results presented below were obtained using the LSD macroscopic energy model with the curvature term (Pomorski and Dudek, 2003) as shown in Eq. (5) and the Nilsson (Nilsson, 1955; Nilsson et al. , 1969) or the Yukawa-folded (Krappe et al., 1979; Moller, 1988) single-particle potentials .

2.2. Shell correction

According to Strutinsky the shell energy is given by the following difference:

$$\delta E_{\mathrm{shell}} = \sum_{occ} 2e_\nu - \widetilde{E}_{\mathrm{Str}}\ , \tag{7}$$

where the sum goes over all occupied single-particle (s.p.) energies e_ν and the second term is the smoothed s.p. energy sum which can be calculated by the Strutinsky prescription (Strutinsky, 1967,1968; Nilsson et al. , 1969). The total shell-energy consists of the proton and neutron contributions. The average sum of the single-particle energies is given by the integral

$$\widetilde{E}_{\mathrm{Str}} = \int_{-\infty}^{\tilde{\lambda}} 2\,e\,\tilde{g}(e)\,de\ , \tag{8}$$

where $\tilde{g}(e)$ is the smooth level density obtained by folding the real spectrum of the single-particle energies

$$g(e) = \sum_\nu \delta(e-e_\nu) \quad\longrightarrow\quad \tilde{g}(e) = \frac{1}{\gamma_S}\sum_\nu j_n\left(\frac{e-e_\nu}{\gamma_S}\right)\ . \tag{9}$$

with Gauss function of the sixth (Nilsson et al. , 1969)

$$j_6(x) = \frac{1}{\sqrt{\pi}}e^{-x^2}\left(\frac{35}{16} - \frac{35}{8}x^2 + \frac{7}{4}x^4 - x^6\right)\ . \tag{10}$$

or higher order correction polynomial. The smearing parameter γ should be of the order of the distance between the major shells to wash out the shell effects in $\widetilde{E}$ and ensure the plateau condition (independence on γ) of the shell energy. One obtains the average Fermi energy $\tilde{\lambda}$ in Eq. (8) from the particle number equation in the system with the smoothed shell structure

$$\mathcal{N} = \int_{-\infty}^{\tilde{\lambda}} 2\,\tilde{g}(e)\,de\ . \tag{11}$$

An alternative to the Strutinsky approach method is averaging of the sinle-particle energy sum over the number of particles (see e.g. (Pomorski , 2004)). This method leads to similar magnitudes of the shell energy corrections for deformed nuclei while for the spherical nuclei absolute values of the negative energy corrections are larger.

2.3. Pairing correction

The pairing correction is defined as the difference between the BCS and the average pairing energy

$$\delta E_{\rm pair} = E_{\rm pair} - \langle E_{\rm pair} \rangle \ . \tag{12}$$

The average pairing correlation energy was supposed to be already contained in the macroscopic part of the binding energy (Myers and Swiatecki, 1966), what is not necessary true what we shall point later. The pairing energy $E_{\rm pair}$ is equal to the difference of the BCS energy and the sum of the energies of the occupied single-particle levels: (Nilsson et al. , 1969)

$$E_{\rm pair} = E_{\rm BCS} - \sum_{occ} 2e_\nu \ , \tag{13}$$

where

$$E_{\rm BCS} = \sum_\nu 2v_\nu^2 e_\nu - G\sum_\nu u_\nu v_\nu - G\sum_\nu v_\nu^4 \tag{14}$$

G is the pairing strength, v_ν and u_ν the occupation and unoccupation BCS factors.

2.4. Potential energy surface

An example of results of the potential energy surface of ^{210}Pu isotope is presented in Fig. 2.4. The calculation was done with the Yukawa-folded (YF) single-particle potential and LSD macroscopic energy using the Modified Funny-Hills shape parametrization of the deformed nucleus shapes (Bartel et al., 2014). The parameter ψ corresponds to the elongation of fissioning nucleus while α' describes the mass asymmetry mode. One can see that the second barrier is significantly reduced by the reflection asymmetry, while the super deformed (SD) and hyper deformed (HD) are on the path which corresponds to the symmetric in mass fission. One has to stress here that the proper choice of the shape parametrization was very important to obtain the shell effects at such very elongated shapes. The right hand side end of the potential energy surface corresponds to the liquid drop scission line.

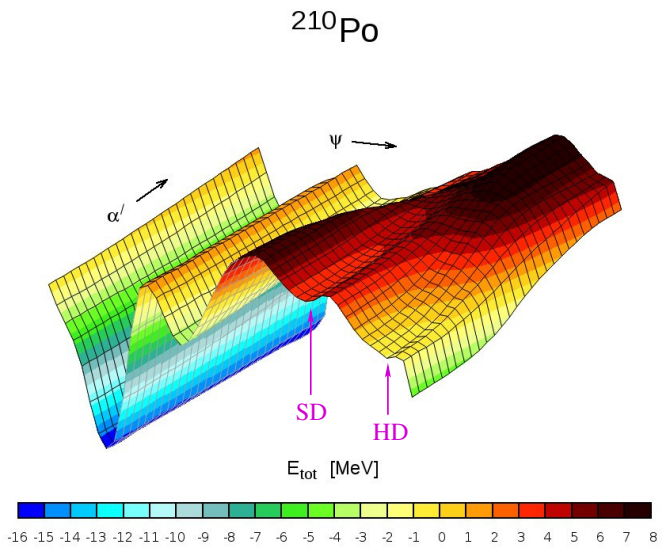

Fig. 1. Potential energy surface of ^{210} Po in elongation ψ and asymmetry α' plane

3. Additive property of the microscopic energy corrections

Let us assume that we are dealing with the almost separated fission fragments. The single-particle potential well of such system is schematically presented in Fig. 2. The bound single-particle levels, which one obtains after diagonalization of the Hamiltonian with such a potential, are already localised in the two wells corresponding to each fission fragment. Only the weakly bound and unboud states have wave functions which are distributed over the whole system.

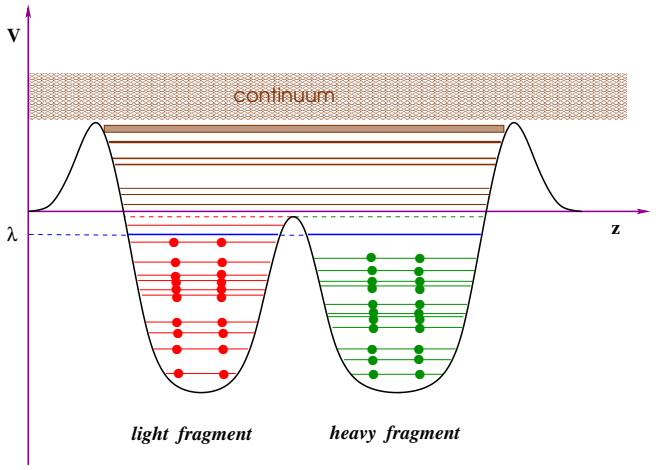

Fig. 2. Schematic plot of a single-particle potential well corresponding to the two almost separated fission fragments.

The common energy spectrum of the bound states can be separated into the levels belonging to the heavy or to the light fragment: $\{e\} \equiv \{e^l, e^h\}$. The both fragments should have the same average Fermi energy (11) as the mother nucleus because the system is not yet fully divided: $\tilde{\lambda}^l = \tilde{\lambda}^h = \tilde{\lambda}$. For such a configuration the following relations can be written:

$$\widetilde{E}_{\rm Str} = \widetilde{E}^l_{\rm Str} + \widetilde{E}^h_{\rm Str} \quad \text{and} \quad \mathcal{N} = \mathcal{N}^l + \mathcal{N}^h \,, \tag{15}$$

So

$$E_{shell} = \sum_{occ} 2e_\nu - \widetilde{E}_{\rm Str} = \sum_{occ} 2e^l_\nu + \sum_{occ} 2e^h_\nu - \tilde{E}^l_{\rm Str} - \tilde{E}^h_{\rm Str} \tag{16}$$

and

$$E_{shell} = E^l_{shell} + E^h_{shell} \,. \tag{17}$$

In case of the pairing energy, the average pairing gaps could be different in the both fragments. Let us consider a nucleus composed of two almost separated fragments in which the pairing correlations are described by the monopole pairing Hamiltonian:

$$\widehat{H} = \widehat{H}_0 + \widehat{H}_{pair} = \sum_\nu e_\nu \left(a^+_\nu a_\nu + a^+_{\bar\nu} a_{\bar\nu}\right) - G \sum_{\nu,\mu} a^+_\nu a^+_{\bar\nu} a_{\bar\mu} a_\mu \,, \tag{18}$$

where a^+_ν and a_ν the particle creation and annihilation operators. One can define the operators of annihilation of a pair of particles in each fragment:

$$\widehat{P}_l = \sum_\nu a^l_{\bar\nu} a^l_\nu \quad \text{and} \quad \widehat{P}_h = \sum_\nu a^h_{\bar\nu} a^h_\nu \,. \tag{19}$$

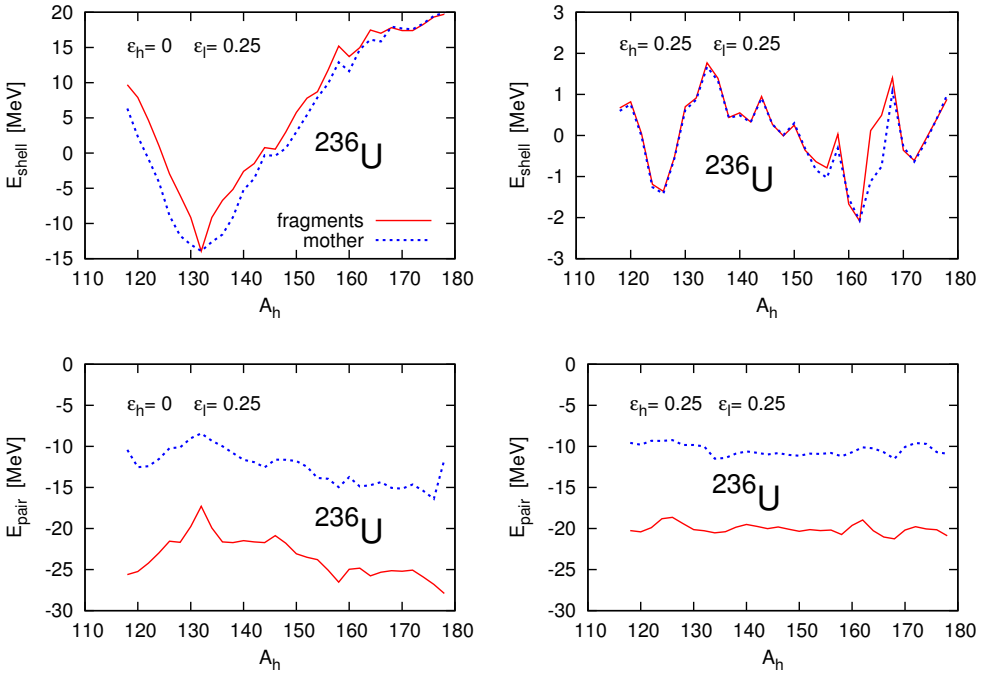

Fig. 3. Sum of the shell energies of fragments (solid line) and the shell energy of the mother nucleus ^{236}U (dotted line) as function of the mass heavy fragment (upper raw). Similar data but for the pairing energy are plotted in the bottom raw. Left column corresponds to spherical heavy fragment and prolate light one while the r.h.s column shows the results when the both fragments are prolate.

and corresponding creation operators $\widehat{P}_l^+ = (\widehat{P}_l)^+$ and $\widehat{P}_h^+ = (\widehat{P}_h)^+$. The single-particle and pairing Hamiltonian in the new operators takes the following form:

$$\widehat{H} = \widehat{H}_0^l + \widehat{H}_0^h - G_l\widehat{P}_l^+\widehat{P}_l - G_h\widehat{P}_h^+\widehat{P}_h - G_{lh}\left(\widehat{P}_l^+\widehat{P}_h + P_h^+\widehat{P}_l\right) . \tag{20}$$

The monopole pairing strength G is in the first approximation proportional to $1/A$, so in the case of the separated fragments the approximation $G_l = G_h = G_{lh} = G$ is not valid any more. One should rather assume: $G_l \geq G_h > G$ and $G_{lh} \approx 0$, where the equality sign is valid for the symmetric fission only.

The BCS equations for almost separated fragments will take the following form:

$$\frac{2}{G} = \sum_\nu \frac{1}{E_\nu} \neq \sum_\nu \frac{1}{E_\nu^l} + \sum_\nu \frac{1}{E_\nu^h} = \frac{2}{G_l} + \frac{2}{G_h} \tag{21}$$

and

$$N = \sum_\nu 2v_\nu^2 = \sum_\nu 2(v_\nu^l)^2 + \sum_\nu 2(v_\nu^h)^2 = N_l + N_h , \tag{22}$$

where

$$E_\nu^l = \sqrt{(e_\nu^l - \lambda_l)^2 + \Delta_l^2} , \quad (v_\nu^l)^2 = \frac{1}{2}\left(1 - \frac{e_i^l - \lambda_l}{E_i^l}\right) , \quad \text{etc.} \tag{23}$$

with $\Delta \neq \Delta_l \neq \Delta_h$ and $\lambda \approx \lambda_l \approx \lambda_h$.

In Fig. 3 the two deformed Nilsson (Nilsson et al. , 1969) wells are used to describe the configuration of the fission fragments. The shell (upper raw) and the pairing (bottom raw) energy of the mother system (dashed line) are compared

with the sum of the shell energies (solid line) of the both fragments of ^{236}U for different mass ratios and two different shapes of the fragments. It is seen in Fig. 3 that the shell energy of the mother nucleus is nearly equal to the sum of the fragments shell energies as it should be according to Eq. (17). The pairing energy is almost doubled in the fragments as can be visible in the two bottom plots in Fig. 3. This is in agreement with results obtained in Ref. (Pomorski and Ivanyuk, 2009) for the systems without shell structure. In the plot we haven't subtracted the average pairing energy nor the pairing diagonal term. The pairing strengths for the mother nucleus and fission fragments was adjusted to the average experimental proton and neutron gaps: $\bar{\Delta}^{(p)}_{\rm exp} = 4.8Z^{-1/3}$ MeV and $\bar{\Delta}^{(n)}_{\rm exp} = 4.8N^{-1/3}$ MeV taken from Ref. (Möller and Nix, 1992).

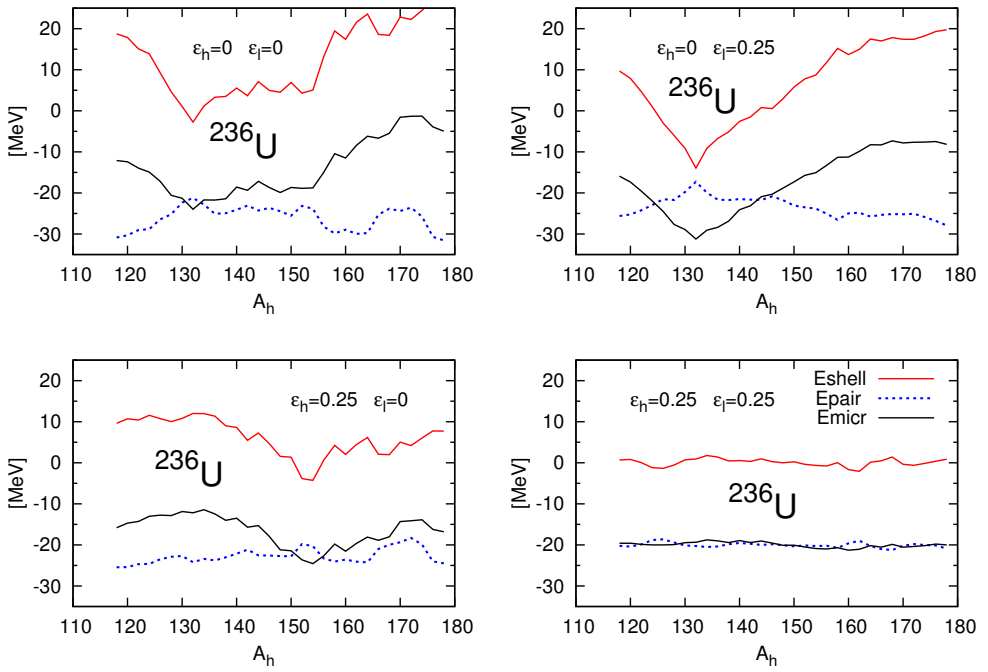

Fig. 4. Shell energy (thin solid line), the sum of the pairing energies of the fragments (dashed line) and the total microscopic energy (thick line) as function of the heavy fragment mass. The results are drawn for four elongations ϵ_h , ϵ_l of heavy and light fragment (written in the plots).

The total value of the microscopic energy as well as its both components $E_{\rm shell}$ and $E_{\rm pair}$ are plotted in Fig. 4 as functions of the heavy fragment mass. Each of four plots corresponds to a different deformations of the fission fragments. We have switched of the pairing interaction between orbitals belonging to different fragments. This can be done automatically when one uses e.g. the δ-pairing force (Krieger, 1990) instead of the monopole pairing interaction

$$V^q(\vec{r}_1,\vec{\sigma}_1;\vec{r}_2,\vec{\sigma}_2) = V_0^q \frac{1-\vec{\sigma}_1\cdot\vec{\sigma}_2}{4}\delta(\vec{r}_1-\vec{r}_2)\,, \quad \text{with} \quad q=n,p\,, \tag{24}$$

where V_0^q is the δ pairing strength, $\vec{\sigma}_1$ and $\vec{\sigma}_2$ denote Pauli matrices. Matrix elements of the δ-pairing force are:

$$V_{i\bar{i}j\bar{j}} = V_0^q \int d^3r \rho_i^q(\vec{r})\rho_j^q(\vec{r})\,, \tag{25}$$

where $\rho_i^q(\vec{r}) = \left|\varphi_i^q(\vec{r})\right|^2$.

It means that the matrix elements (25) vanish when the orbits ϕ_i^q and ϕ_j^q belong to the different fragments. One obtains similar effect in case of the Gogny interaction (Gogny, 1975) frequently used in the self-consistent Hartee-Fock-Bogolubov calculations.

4. Influence of the congruence and the average pairing energies on the fission barrier heights

In the macroscopic-microscopic model one usually assumes that the average pairing energy is contained in the macroscopic part of the binding energy. To check the validity of this assumption one has evaluated in Ref. (Pomorski and Ivanyuk, 2009) the average monopole pairing energy of nuclei from different mass regions at small deformations corresponding to the ground state and at the scission configurations. The proportional to v_ν^4 term in Eq. 14 was taken into account when evaluating the pairing energy.

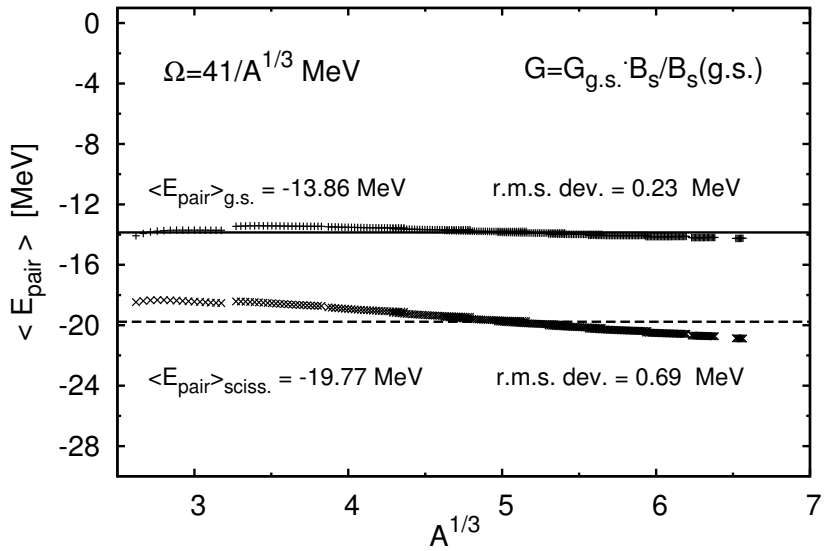

Fig. 5. Average pairing energy of nuclei at the ground state and at the scission point in function of $A^{1/3}$. (After (Pomorski and Ivanyuk, 2009)).

The results are presented in Fig. 5. One can see that the average pairing energy in the ground state is almost A-independent and approximately equal to -14 MeV. This result means that the average-pairing should be doubled when two fission fragments are born from the mother nucleus. There is no mechanism in the macroscopic-microscopic model which can give this effect. The only remedy is to assume that the average-pairing energy should not be included into the macroscopic energy. In addition one has to take the deformation dependent monopole-pairing strength or more complex pairing force as discussed in the previous section. The taking into account the fluctuative part of the pairing energy $\delta E_{\rm pair}$ only leads to a systematic error in the deformation dependence of the macroscopic-microscopic energy. One has to add to the macroscopic energy $E_{\rm macr}$ the whole pairing energy (13) not only its fluctuating part in order to get proper estimates of the binding energy at the saddle-point as well as at the scission configuration.

It was shown in Ref. (Pomorski and Ivanyuk, 2009) that the proportional to the surface monopole pairing strength ($G \sim S$) can roughly give the doubling effect of the pairing energy at scission. It is seen in Fig. 5 that the magnitude of $< E_{\rm pair} >$ evaluated with $G \sim S$ at the scission configuration is much larger (almost twice for the heaviest nuclei) than in the ground-state.

Similar effect but for the congruence (Wigner) energy was already noticed in Ref. (Myers and Swiatecki, 1997), where one has assumed that the congruence energy at the scission point is twice as large as in the ground state. The effect of deformation dependent congruence and average pairing energy on the fission barrier heights was discussed in Ref. (Pomorski and Ivanyuk, 2009) and is shown in Fig. 6 for Br to Cf isotopes. It is seen in Fig. 6 that the deformation dependent average-pairing and congruence energies significantly approaches the estimates of the fission barrier heights to their measured values (Pomorski and Ivanyuk, 2009).

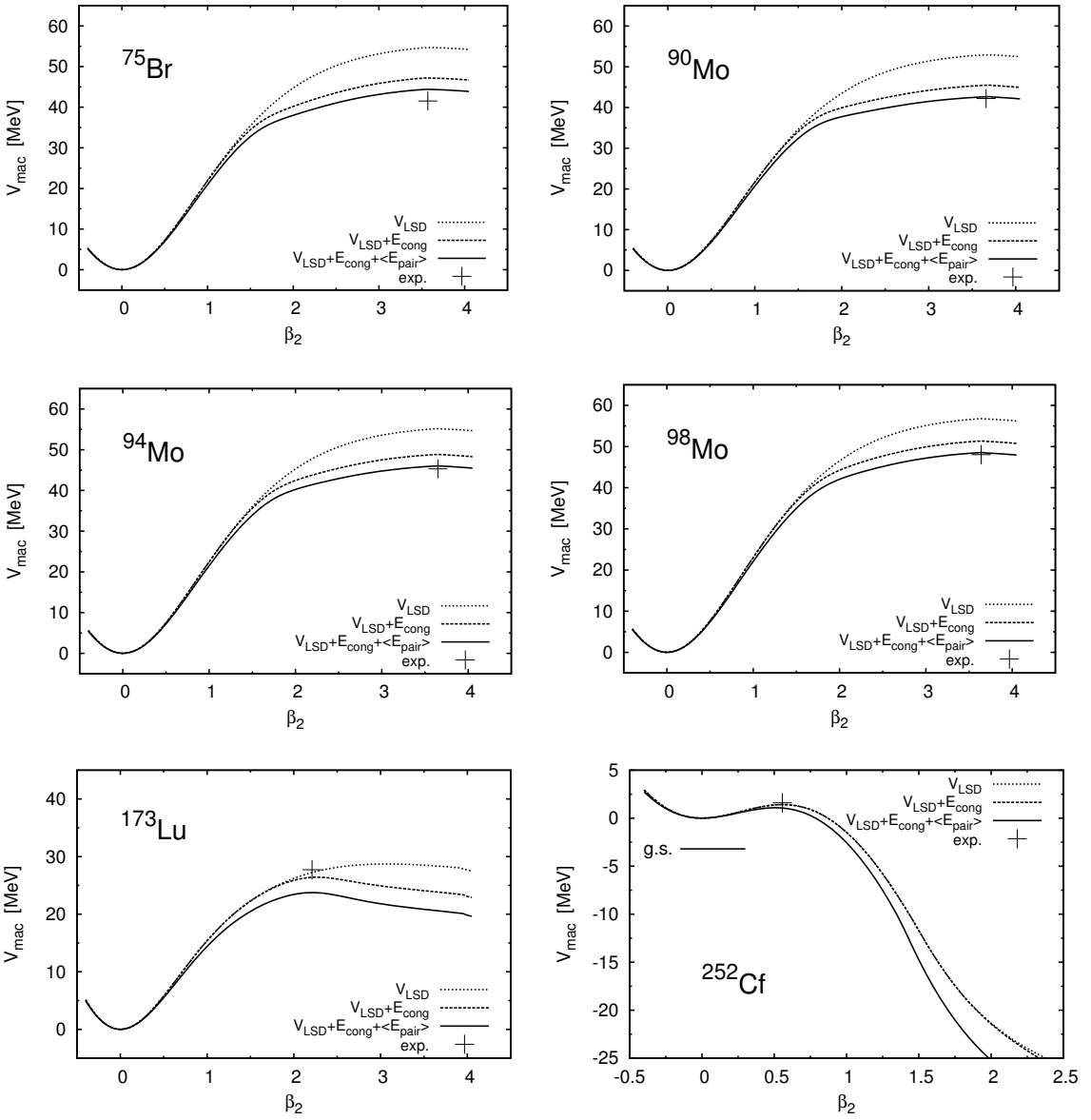

Fig. 6. The macroscopic fission barrier of ^{75}Ba to ^{252}Cf isotopes as function of the quadrupole deformation of nuclei. The barriers are evaluated using the LSD energy (dotted lines) and the deformation dependent congruence (dashed lines) and average-pairing terms (solid lines). The crosses correspond to the experimental fission barrier heights reduced by the microscopic effects at the ground-state according to the topographical theorem (Myers and Swiatecki, 1996).

The barrier heights were estimated using the topographical theorem of Swiatecki in which one assumes that at the binding energy of nucleus at the saddle is mostly determined by the macroscopic part of the binding energy. The quality of this approximation can be seen in Fig. 7, where the experimental fission barrier heights of 18 actinide nuclei are compared to their estimates in which the LSD macroscopic mass formula was used to evaluate the mass of nuclei

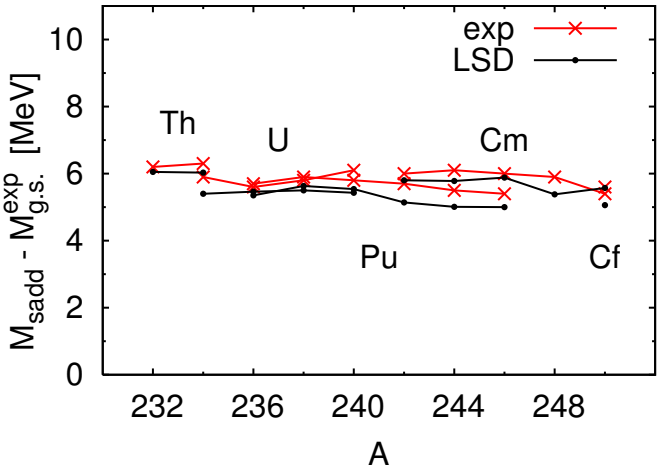

Fig. 7. The LSD fission barrier barrier heights of actinide nuclei points compaers with the data (crosses). The topographical theorem (Myers and Swiatecki, 1996) was used to obtain these estimates.

at the saddle point. All estimates except one (^{252}Cf) are slightly below the data (r.m.s. 310 keV) what leaves a place for the small unwashed shell effects at the saddle.

5. Spontaneous fission

The spontaneous–fission half–life is inversely proportional to the probability P of penetration through the fission barrier (confer e.g. (Krappe and Pomorski, 2012):

$$T^{\rm sf}_{1/2} = \frac{\ln 2}{n}\frac{1}{P}\ , \tag{26}$$

where n is the number of assaults of the nucleus on the fission barrier per time unit. The number of assaults is given by the frequency of zero–point vibration of the nucleus in the fission mode direction. Using the one-dimensional WKB approximation one obtains the following equation for the penetration probability:

$$P = \frac{1}{1+\exp 2S(L)}\ , \tag{27}$$

where $S(L)$ is the action–integral calculated along a fission path $L(s)$ in the multi–dimensional space of collective coordinates $\{q_i\}$

$$S(L) = \int_{s_1}^{s_2}\left\{\frac{2}{\hbar^2}B_{\rm eff}(s)[V(s)-E_{\rm g.s.}]\right\}^{1/2} ds\ . \tag{28}$$

Here $V(s)$ is the collective potential and $E_{\rm g.s.}$ is the ground state energy of nucleus. An effective inertia associated with the fission mode along the path $L(s)$ is:

$$B_{\rm eff}(s) = \sum_{k,l} B_{kl}\frac{dq_k}{ds}\frac{dq_l}{ds}\ , \tag{29}$$

where B_{kl} are the q_k and q_l components of the inertia tensor and ds denotes the element of the path length in the multi-dimensional space of collective coordinates $\{q_i\}$. The integration limits s_1 and s_2 correspond to the classical turning points.

Encouraged by the good results for the α-decay and the cluster radioactivity half-lives obtained within the Gamow theory (Zdeb et al., 2013), we are going to check another simple model for the spontaneous fission half-lives proposed in 1955 by Swiatecki (Swiatecki, 1955). He has who proposed a simple phenomenological relation between the half-lives and the experimental mass deviations from their liquid drop estimates. The crucial ingredient of the model is the liquid drop type formula which should reproduce well both the average binding energies of nuclei and the fission barrier heights. The LSD model seems to fulfill the both criteria.

Let us consider one dimensional fission barrier along the least-action (dynamic) trajectory which corresponds to a path in the multidimensional deformation parameter space which minimizes the integral S (28). Assuming that the fission path is parametrised by a collective coordinate s one can evaluate the potential $V(s)$ and the mass parameter $B_{ss}(s)$ corresponding to this path. The fluctuations of the inertia B_{ss} along the least-action trajectory becomes smaller and smaller when one increase the number of collective coordinates. Especially the collective pairing degrees of freedom significantly wash out the fluctuations of the inertia function (Staszczak et al., 1989).

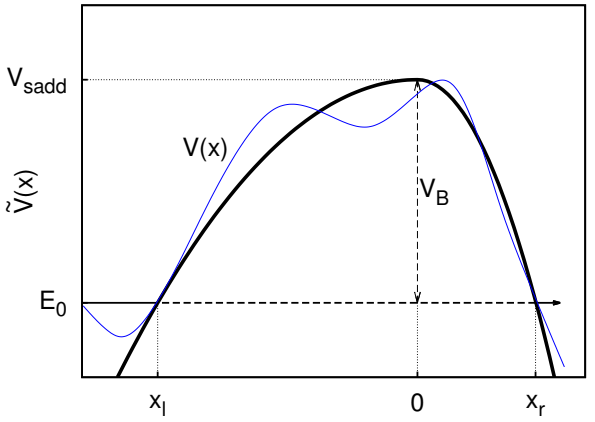

Fig. 8. Schematic plot of a fission barrier. Two, at the saddle point, smoothly joined inverted parabolas approximate the barrier form.

A simple transformation:

$$\mathrm{x}(s) = \int_{s_{\mathrm{sadd}}}^{s} \sqrt{\frac{B_{ss}(s')}{m}}\, ds' \ , \tag{30}$$

brings us to the new coordinate $\mathrm{x}(s)$ in which the inertia becomes constant $B_{\mathrm{xx}} = m$. The lower integration limit in Eq. (30) are chosen in such a way that x=0 corresponds to the saddle point s_{sadd}. The collective potential in the new coordinate, schematically presented in Fig. 8, can be approximated by the two inverted parabolas of different stiffness C_l and C_r having the maximum at the saddle point:

$$\widetilde{V}(\mathrm{x}) = \begin{cases} V_{\mathrm{sadd}} - \frac{1}{2}\, C_l\, \mathrm{x}^2 & \text{for} \quad \mathrm{x} < 0 \ , \\ V_{\mathrm{sadd}} - \frac{1}{2}\, C_r\, \mathrm{x}^2 & \text{for} \quad \mathrm{x} > 0 \ , \end{cases} \tag{31}$$

The stiffnesses of the $\widetilde{V}$ potential are chosen in such a way that the action-integral S (28) becomes equal:

$$S = \int_{-\mathrm{x}'_l}^{\mathrm{x}'_r} \sqrt{\frac{2m}{\hbar^2}[V(\mathrm{x}) - E_0]}\, d\mathrm{x} = \int_{-\mathrm{x}_l}^{\mathrm{x}_r} \sqrt{\frac{2m}{\hbar^2}[\widetilde{V}(\mathrm{x}) - E_0]}\, d\mathrm{x} \tag{32}$$

where pairs $(-\mathrm{x}'_l, \mathrm{x}'_r)$ and $(-\mathrm{x}_l, \mathrm{x}_r)$ are classical left and right turning points for the true and approximative potential respectively. The last integral in Eq. (32) can be rewritten as

$$S = \sqrt{\frac{2m}{\hbar^2}} \left\{ \int_0^{\mathrm{x}_l} \sqrt{V_B - \frac{C_l \mathrm{x}^2}{2}}\, d\mathrm{x} + \int_0^{\mathrm{x}_r} \sqrt{V_B - \frac{C_r \mathrm{x}^2}{2}}\, d\mathrm{x} \right\},$$

where $V_B = V_{\rm sadd} - E_0$ is the fission barrier height.

After a small algebra the action integral becomes

$$S = \frac{\pi}{2\hbar} V_B \left(\sqrt{\frac{m}{C_l}} + \sqrt{\frac{m}{C_r}} \right) = \frac{\pi}{\hbar} V_B \frac{\omega_l + \omega_r}{2\omega_l \omega_r} \ , \tag{33}$$

where $\omega_l = \sqrt{C_l/m}$ and $\omega_r = \sqrt{C_r/m}$ are frequencies of the left and right (inverted) oscillator respectively. Introducing the average oscillator frequency

$$\widetilde{\omega} = \frac{2\omega_l \omega_r}{\omega_l + \omega_r}\,, \tag{34}$$

one can bring the action integral to the following form:

$$S = \frac{2V_B}{\hbar\widetilde{\omega}}\,. \tag{35}$$

In our approximation the action integral is proportional to the fission barrier height measured in the energy quanta of the harmonic oscillator which approximates the fission barrier form. For the action-integral $S > 1$ the logarithm of the spontaneous fission half-lives (26) can written as

$$\log(T^{\rm sf}_{1/2}/y) = 2S - \log(n) - 0.3665 \tag{36}$$

where n is the number of assaults of nucleus on the fission barrier per year (y) and the constant 0.3665=log[log(2)]. Having in mind that according to the topographical theorem the fission barrier height is $V_B = M^{\rm sadd}_{\rm LSD} - M^{g.s.}_{exp}$ and making use of the relation (35) one can rewrite the last equation as follows:

$$\log(T^{\rm sf}_{1/2}/y) + \frac{4\delta M}{\hbar\tilde{\omega}} = \frac{4V^{\rm LSD}_B}{\hbar\tilde{\omega}} - \log(n) - 0.3665\,, \tag{37}$$

where

$$\delta M = M^{\rm g.s.}_{\rm exp} - M^{\rm sph}_{\rm LSD} \qquad \text{and} \qquad V^{\rm LSD}_B = M^{\rm sadd}_{\rm LSD} - M^{\rm sph}_{\rm LSD} \tag{38}$$

are the ground state microscopic energy correction and the liquid drop fission barrier height receptively.
The right hand side of Eq. (37) is a very smooth function of nucleon numbers as it is defined only by global properties of nucleus. Note, that the derived equation has the same structure as the phenomenological formula in Ref. (Swiatecki, 1955).

The liquid drop barrier height of actinides decreases almost linearly in function of Z from 4.3 MeV for $Z = 90$ to 0 for $Z \geq 103$ (Ivanyuk and Pomorski, 2009). The fission barrier of finite height appears in the super-heavy nuclei mostly due to the shell effects in the ground state. The smooth dependence of logarithms of spontaneous fission half-lives, corrected by the ground state shell-plus-pairing effects (k=7.7/MeV), on the LSD fission barrier heights, is shown in Fig. 9 for even-even (e-e), odd A (o-A) and odd-odd (o-o) nuclei (Zdeb et al., 2015). The data for e-e isotopes lie very close to the straight line what validates Eq. (37). The data for o-A and o-o are above this line, what is due to the specialization energy which increases the fission barrier heights.

In Fig. 10 the spontaneous fission half-lives for even-even nuclei in function of Z^2/A are shown (Zdeb et al., 2015). They are fitted by the 3 parameter formula which implicates from Eq. (37) and it is very close to that proposed in Ref. (Swiatecki, 1955):

$$\log_{10}\left(\frac{T^{\rm sf}_{1/2}}{y}\right) + k\delta M = a\,Z + b + h\,[\mathrm{mod}(Z,2) + \mathrm{mod}(N,2)] \tag{39}$$

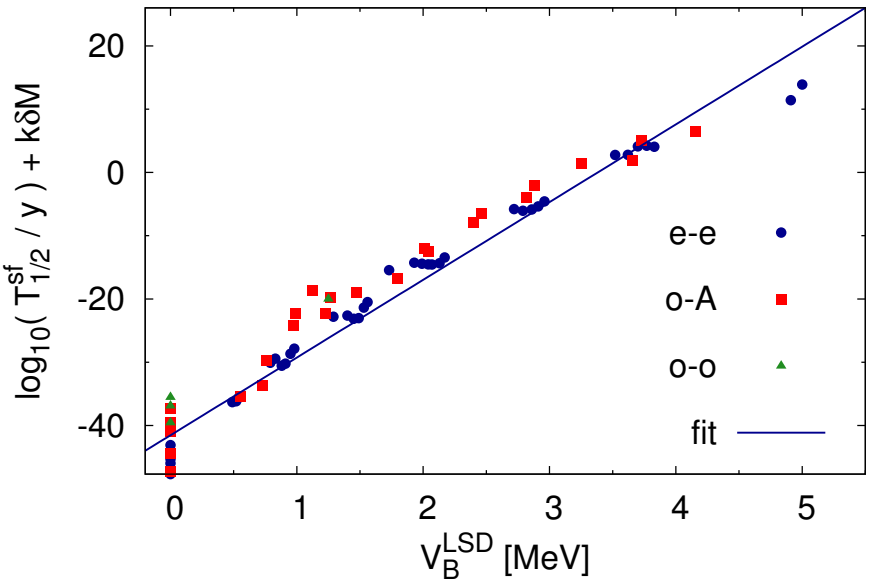

Fig. 9. Logarithms of the observed spontaneous fission half-lives corrected by $7.7\delta M$ as a function of liquid drop barrier height.

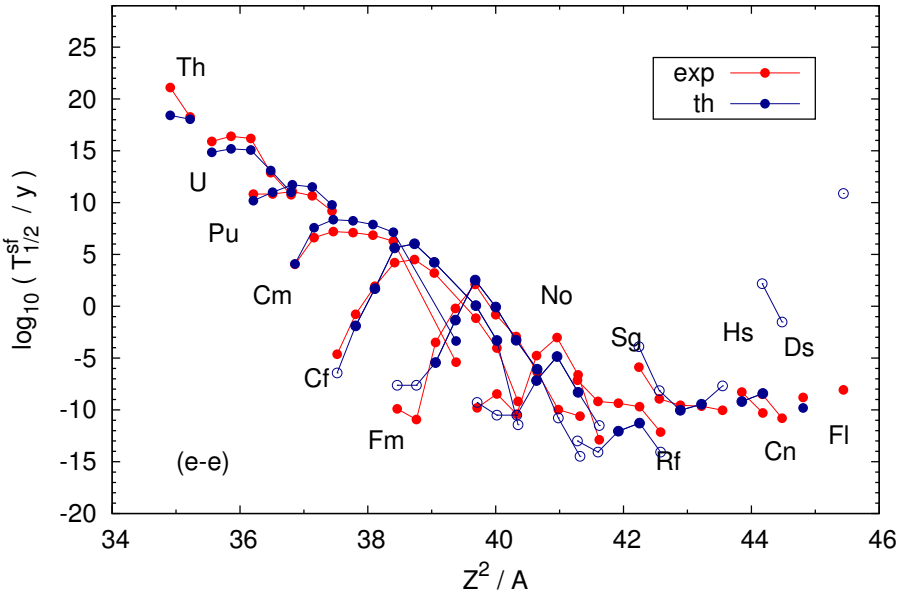

Fig. 10. Logarithms of the observed spontaneous fission half-lives and their estimates by formula (39).

with the adjusted to the data constants $a = 4.1$, $b = 380.2$, $k = 7.7$/MeV and odd-particle hindrance factor $h = 2.5$. The r.m.s. deviation of $T^{sf}_{1/2}$ for the even-even nuclei with $Z \leq 104$ is 1.2 only. The agreements for the odd-A and odd-odd systems are of similar quality.

We have shown here that the spontaneous fission half-lives are determined mostly by the microscopic (shell plus pairing) effects in the ground state and depend on the global properties of the macroscopic fission barrier like its height and width. The microscopic energy corrections at larger deformations have only a tiny influence on the fission probability. In other words: the systematics of fission life-times depends mostly on the ground-state properties of nuclei.

6. Conclusions

The following conclusions can be drawn form our investigations:

- The sum of shell energies of the fission fragments is close to the shell energy of the mother system.
- The sum of pairing energies of the fission fragments could be different from the pairing energy evaluated for the common system.
- The deformation dependent congruence (Wigner) energy and the pairing strength proportional to the nuclear surface improve the estimates of the barrier heights of the light nuclei.
- The average pairing energy of fissioning nucleus should grow with deformation to the double value at the scission point.
- Lublin Strasbourg Drop describes well masses of all isotopes both in the ground state and saddle points.
- The spontaneous fission half-lives are mostly determined by the ground state shell effects
- Binuclear structure can appear in Th or lighter elements which have a very long flat fission barrier allowing for creation of the local minima corresponding to the super- and hyper-deformed shapes.

Acknowledgements

The work was partly supported by the Polish National Science Centre, grant No. 2013/11/B/ST2/04087.

References

Bardeen, J., Cooper, L. N., Schrieffer, J. R., 1957. Theory of Superconductivity, Physical Review 108, 1175–1204.

Bartel, J., Nerlo-Pomorska, B., Pomorski, K., Schmitt, C., 2014. The potential energy surface of 240Pu around scission, Physica Scripta 89, 054003,1–5.

Bartel, J., Dobrowolski, A., Pomorski, K., 2007. Saddle-point masses of even-even actinide nuclei, Int. Journal Modern Physics E16, 459–473.

Bohr, N., Wheeler, J. A., 1939. The Mechanism of Nuclear Fission, Physical Review 56, 426–450.

Bolsterli, M., Fiset, E. O., Nix, J. R., Norton, L., 1972. New Calculation of Fission Barrier for Heavy and Superheavy nuclei, Physical Review C 5, 1050–1078.

Dobrowolski, A., Pomorski, K., Bartel, J., 2007. Fission barriers in a macroscopic-microscopic model, Physical Review C75, 024013, 1–17.

Gogny, D., 1975. in "*Nuclear Self Consistent Fields*", Ripka G. and Porneuf M. (Eds.), North Holland, Amsterdam, p. 333.

Hahn, O., Straßmann, F., 1939. Über den Nachweis und Verhalten der bei der Bestrahlung des Urans mittels Neutronen entstehenden Erdalkalimetale, Naturwissenschaften 27, 11–15.

Ivanyuk, F. A., Pomorski, K., 2009. Optimal shapes and fission barriers of nuclei within the liquid drop model, Physical Review C 79, 054327, 1–11.

Krappe, H. J., Pomorski, K., *Theory of Nuclear Fission*, Springer Verlag, Heidelberg, 2012.

Krappe, H. J., Nix, J. R., Sierk, A. J., 1979. Unified nuclear potential for heavy-ion elastic scattering, fusion, fission, and ground-state masses and deformations, Physical Review C 20, 992–1013.

Krieger, S. J., Bonche, P., Flocard, H., Quentin, P., and Weiss, M., 1990. An improved pairing interaction for mean field calculations using Skyrme potentials, Nuclear Physics A517, 275-284.

Meitner, L., Frisch, O. R., 1939. Disintegration of Uranium by Neutrons: a New Type of Nuclear Reaction, Nature 143, 239–240.

Möller, P., Myers, W. D., Swiatecki, W. J., Treiner, J., 1988. Nuclear mass formula within a finite-range droplet model and folded-Yukawa single-particle potential, Atomic Data and Nuclear Data Tables 39, 225.

Möller, P., Nix, J. R., 1992. Nuclear pairing model, Nuclear Physics A536, 20–60 .

Möller, P., Nix, J. R., 1992. The Coulomb redistribution energy by a as revealed refined study of nuclear masses, Nuclear Physics A536, 61–71.

Myers, W. D., Swiatecki, W. J., 1966, Nuclear Masses and Deformations, Nuclear Physics 81, 1–60.

Myers, W. D., Swiatecki, W. J., 1969. Average Nuclear Properties, Annals of Physics 55, 395–505; ibid. 1974. Nuclear Droplet Model for Arbitrary Shapes, Annals of Physics 84, 186–210.

Myers, W. D., Swiatecki, W. J., 1996. Nuclear properties according to the Thomas-Fermi model, Nuclear Physics A601, 141–167.

Myers, W. D., Swiatecki, W. J., 1997. The congruence energy: a contribution to nuclear masses, deformation energies and fission barriers, Nuclear Physics A612, 249–261.

Nilsson, S. G., 1955. Binding states of individual nucleons in strongly deformed nuclei, Det Kongelige Danske Videnskabernes Selskab Matematisk-fysiske Meddelelser 29, no. 16, 1–70.

Nilsson, S. G., Tsang, C. F., Sobiczewski, A., Szymanski, Z., Wycech, S., Gustafson, C., Lamm, I. L., Möller, P., and Nilsson, B., 1969. On the nuclear structure and stability of heavy and superheavy elements, Nuclear Physics A131, 1–66.

Pomorski, K., Dudek, J., 2003. Nuclear liquid-drop model and surface-curvature effects, Physical Review C 67, 044316, 1–13.

Pomorski, K., 2004. Particle number conserving shell-correction method, Physical Review C 70, 044306, 1–10.

Pomorski, K., Dudek, J., 2004. Fission barriers within the liquid drop model with the surface-curvature term, Int. Journal Modern Physics E13, 107–112 .

Pomorski, K., Ivanyuk, F., 2009. Pairing correlations and fission barrier heights, Int. Journal Modern Physics E18, 900–906.

Staszczak, A., Pilat, S., Pomorski, K., 1989. Influence of the Pairing Vibrations on Spontaneous Fission Probability, Nuclear Physics. A504, 589–604.

Strutinsky, V. M., 1967. Shell effects in nuclear masses and deformation energies , Nuclear Physics, A95, 420–442 ; 1968. Shells in deformed nuclei, Nuclear Physics A122, 1–33.

Swiatecki, W. J., 1955. Systematics of Spontaneous fission Half-Lives, Physical Review 100, 937–938.

Woods, R. D., Saxon, D. S., 1954. Diffuse Surface Optical Model for Nucleon-Nuclei Scattering Physical Review 95, 577–578.

Zdeb, A., Warda, M., Pomorski, K., 2013, Half-lives for alpha and cluster radioactivity within a Gamow-like model, Physical Review C 87, 024308, 1–5.

Zdeb, A., Warda, M., Pomorski, K., 2014, On spontaneous fission and α-decay half-lives of atomic nuclei, Physica Scripta, submitted for publication.